American Mineralogist, Volume 94, pages 200–203, 2009

LETTER

Octahedral cation distribution in palygorskite

GEORGIOS D. CHRYSSIKOS,[1,*] VASSILIS GIONIS,[1] GEORGE H. KACANDES,[2] ELIZABETH T. STATHOPOULOU,[1,†] MERCEDES SUÁREZ,[3] EMILIA GARCÍA-ROMERO,[4] AND MANUEL SÁNCHEZ DEL RÍO[5]

[1]Theoretical and Physical Chemistry Institute, National Hellenic Research Foundation, 48 Vassileos Constantinou Avenue, 11635 Athens, Greece
[2]Geohellas S.A., 60 Zephyrou Street, 17564 Athens, Greece
[3]Departamento de Geología, Universidad de Salamanca, 37008 Salamanca, Spain
[4]Departamento de Cristalografía y Mineralogía, Universidad Complutense de Madrid, 28040 Madrid, Spain
[5]European Synchrotron Radiation Facility, BP 220 38043 Grenoble Cedex, France

ABSTRACT

The OH speciation of 18 palygorskite samples from various localities were evaluated by near infrared spectroscopy (NIR) and compared to the corresponding octahedral composition derived from independent, single-particle analytical electron microscopy (AEM). NIR gives evidence for dioctahedral-like (AlAlOH, $AlFe^{3+}OH$, $Fe^{3+}Fe^{3+}OH$) and trioctahedral-like (Mg_3OH) species. Therefore, palygorskite can be approximated by the formula $y Mg_5 Si_8O_{20}(OH)_2 \cdot (1 - y)[x Mg_2Fe_2 \cdot (1 - x) Mg_2Al_2] Si_8O_{20}(OH)_2$, where x is the Fe content of the dioctahedral component, and y is the trioctahedral fraction. The values of x estimated from the NIR data are in excellent agreement with the $Fe/(^{VI}Al + Fe)$ ratio from AEM ($R^2 = 0.98$, $\sigma = 0.03$), thus suggesting that all octahedral Al and Fe in palygorskite participate in M2M2OH (dioctahedral-like) arrangements. Furthermore, y values from AEM can be compared to NIR ($R^2 = 0.90$ and $\sigma = 0.05$) after calibrating the relative intensity of the Mg_3OH vs. $(Al,Fe)_2OH$ overtone bands using AEM data. The agreement between the spectroscopic and analytical data are excellent. The data show that Fe^{3+} for Al substitution varies continuously in the analyzed samples over a broad range ($0 < x < 0.7$), suggesting that fully ferric dioctahedral palygorskites ($x = 1$) may exist. On the other hand, the observed upper trioctahedral limit of $y = 0.50$ calls for the detailed structural comparison of Mg-rich palygorskite with sepiolite.

Keywords: Palygorskite, Fe-rich, Mg-rich, structure, near infrared spectroscopy, trioctahedral, dioctahedral, composition, AEM, sepiolite

INTRODUCTION

Palygorskite is a common mineral in dusts and soils (Singer 1989) and the key ingredient of the ancient Mesoamerican pigment known as Maya Blue (Van Olphen 1966). It is a phyllosilicate with a 2:1 layer having periodic inversions of the tetrahedral sheet after every two silicate "chains" to form "ribbons." The octahedral sheet is thus discontinuous and a channel-like structure forms (Giustetto and Chiari 2004; Post and Heaney 2008). Palygorskite is chemically more complex than sepiolite, a magnesian trioctahedral phyllosilicate of the same family, owing to octahedral cation substitutions involving Mg, Al, and Fe (Paquet et al. 1987; Galán and Carretero 1999; Suárez et al. 2007). The octahedral sheet of palygorskite (Fig. 1) can be dioctahedral, consisting of M2M2OH groups and vacant M1 sites, or trioctahedral with M1M2M2OH groups, whereas the edge M3 sites fulfill their coordination with H_2O.

Following the pioneering work of Serna et al. (1977), several studies have employed mid-infrared spectroscopy to identify the environment around OH species in palygorskite (Chahi et al. 2002; García-Romero et al. 2004; Cai et al. 2007). Based on these studies, there is growing consensus that the M3 sites are occupied by Mg, whereas Al and Fe^{3+} populate M2 sites and excess Mg may occupy both M2 and M1 sites (Suárez and García-Romero 2006). However, difficulties from overlap between the OH and H_2O stretching modes, or from associated minerals interfering with the OH deformation modes, place limits on a detailed structural description of palygorskite.

In a mid- and near-infrared (NIR) investigation of palygorskite, Gionis et al. (2006) showed that NIR can separate the OH from H_2O modes, and is less prone to interference from accessory minerals (silicates, carbonates, etc.). Four OH stretching overtone modes representing three M2M2OH (i.e., AlAlOH, $AlFe^{3+}OH$, $Fe^{3+}Fe^{3+}OH$) and one M1M2M2OH (i.e., Mg_3OH) species were identified in second derivative NIR spectra. A subsequent NIR investigation of more than 300 samples from the Pefkaki deposit (W. Macedonia, Greece) failed to identify additional types of structural OH environments in palygorskite (Gionis et al. 2007). Therefore, the composition of palygorskite was approximated by the formula $y Mg_5 Si_8O_{20}(OH)_2 \cdot (1 - y)[x Mg_2Fe_2 \cdot (1 - x) Mg_2Al_2] Si_8O_{20}(OH)_2$, where x represents the Fe content of the dioctahedral component, and y is the trioctahedral fraction. The value of x, determined by measuring the relative intensities of the three M2M2OH stretching overtone modes, ranged between 0.3 and 0.7. The value of y was estimated indirectly by subtracting the

* E-mail: gdchryss@eie.gr
† Present address: Department of Historical Geology and Palaeontology, Subfaculty of Geology and Geoenvironment, University of Athens, Panepistimiopolis, 15784, Zografou, Athens, Greece.

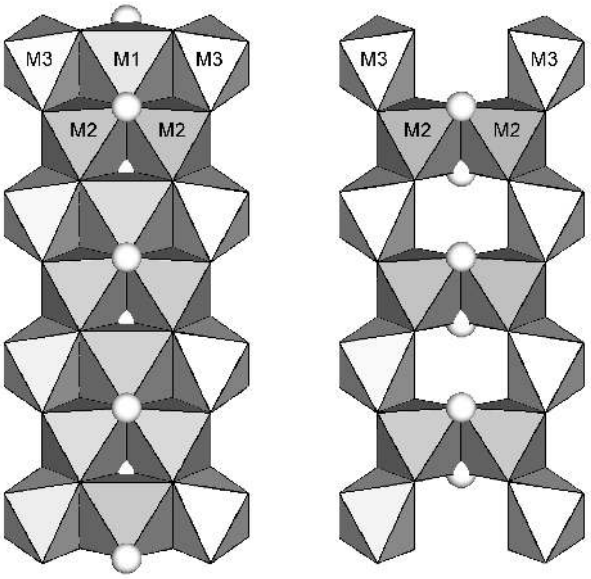

FIGURE 1. Trioctahedral (left) and dioctahedral (right) sheet of palygorskite with the OH groups in M1M2M2 and M2M2 environments shown as spheres.

amount of dioctahedral palygorskite (determined by NIR on the basis of the sum intensity of the M2M2OH overtones), from the total amount of palygorskite estimated from the intensity of the d_{110} reflection in a powder X-ray diffraction (XRD) pattern. Values of y ranged from 0 to 0.55 (Gionis et al. 2007).

Here, we determine if the above simplified palygorskite formula is compatible with chemical analysis. To do this, we examined 18 palygorskite samples and compared the results of NIR analysis to chemical data obtained on single particles by analytical electron microscopy (AEM).

MATERIALS AND EXPERIMENTAL METHODS

Seven studied palygorskite samples are reported by Suárez et al. (2007): LIL and BOT (Lisbon volcanic complex, Portugal), YUC (Ticul, Yucatán, Mexico), BER (Bercimuel, Segovia, Spain), ESQ (Esquivias, Madrid, Spain), TRA (Los Trancos, Almería, Spain), and TOR (Torrejón el Rubio, Cáceres, Spain). Two samples are from Esquivias, (ESQ-2) and Pics Crossing, Australia (PIC). Nine samples (GR series) are handpicked from the Pefkaki deposit, W. Macedonia, Greece. Samples GR-1 and GR-2 were reported by Gionis et al. (2006, 2007). All samples were of high purity with d_{110} values ranging from 10.46 Å (LIL) to 10.67 Å (GR-2, GR-9). Minerals present as impurities include calcite, dolomite, and quartz, and the GR samples contain small amounts of saponitic smectite and/or serpentine.

The experimental conditions and data analysis for the AEM and NIR measurements are discussed by Suárez et al. (2007), García-Romero et al. (2007), and Gionis et al. (2007). In brief, the NIR spectra were measured on powdered samples (70–100 mg) on a Fourier transform instrument (Vector 22N by Bruker Optics) equipped with an integrating sphere accessory. The spectra represent an average of 200 scans measured at a resolution of 4 cm^{-1}, using Blackman-Harris 3-term apodization and a zero filling factor of 2. Second derivatives of the NIR absorption were calculated with the Savitzky-Golay algorithm with 13-point smoothing. TEM observations and AEM analysis of each sample, deposited from suspensions on microscope grids with collodion, were performed in two different laboratories ("Luis Bru," Complutense University of Madrid and CIC, University of Granada). The AEM results represent the average of 25–100 single particle measurements per sample. Synthetic clays were used as reference to test the validity of the K-factors employed in the calculations.

RESULTS AND DISCUSSION

The octahedral composition of each palygorskite sample by AEM (Table 1) shows large variations in Al (0.37–1.91), Fe (0.04–0.99), and Mg (1.98–3.34) per $O_{20}(OH)_2$. Table 1 includes compositional parameters x = Fe/(Al + Fe) and y = [2Mg – 2(Al + Fe)]/[2Mg + 3(Al + Fe)], as defined above. Thus, the AEM data indicate that the substitution of Al by Fe in the M2 sites varies from nearly zero (LIL) to ca. 70% (GR-9), whereas the fraction

TABLE 1. Tetrahedral and octahedral cations of palygorskite per $O_{20}(OH)_2$, by AEM

	AEM								NIR		
Sample	Si	^{IV}Al	^{VI}Al	Fe^{3+}	Mg	x	y	$y/(1-y)$	x_{NIR}	K_{NIR}	y_{NIR}
LIL*	8.02(4)	0.00(1)	1.91(5)	0.04(2)	2.01(8)	0.02	0.01	0.01	0.00	0.02	0.00
BOT*	7.98(6)	0.02(5)	1.61(6)	0.16(1)	2.27(9)	0.09	0.10	0.11	0.10	0.14	0.09
TRA*	8.02(4)	0.00(2)	1.20(11)	0.16(3)	2.89(11)	0.12	0.31	0.45	0.13	0.23	0.14
ESQ*	7.87(9)	0.13(9)	1.04(11)	0.20(6)	3.11(26)	0.16	0.38	0.60	0.13	0.55	0.28
ESQ-2	7.95(13)	0.08(8)	0.92(19)	0.14(9)	3.34(32)	0.13	0.46	0.86	0.15	1.27	0. 48
YUC*	7.85(13)	0.15(12)	1.57(20)	0.24(5)	2.21(22)	0.13	0.08	0.09	0.15	0.16	0.10
BER*	7.90(12)	0.10(7)	1.60(20)	0.39(4)	1.98(25)	0.20	0.00	0.00	0.21	0.01	0.01
TOR*	7.91(7)	0.09(5)	1.48(6)	0.37(4)	2.25(6)	0.20	0.08	0.09	0.20	0.08	0.06
PIC	7.95(6)	0.06(5)	1.29(7)	0.47(9)	2.23(7)	0.27	0.10	0.11	0.27	0.14	0.09
GR-0	7.79(11)	0.21(11)	1.14(6)	0.67(6)	2.25(10)	0.37	0.09	0.10	0.36	0.11	0.08
GR-1	7.96(11)	0.06(6)	1.00(20)	0.90(17)	1.99(43)	0.47	0.02	0.02	0.50	0.10	0.07
GR-2	7.87(28)	0.16(28)	0.62(20)	0.56(17)	3.16(43)	0.47	0.40	0.67	0.47	1.15	0.45
GR-3	7.97(6)	0.04(5)	0.67(12)	0.89(7)	2.57(21)	0.57	0.21	0.26	0.60	0.25	0.15
GR-4	7.89(11)	0.11(9)	0.63(11)	0.99(10)	2.45(19)	0.61	0.17	0.20	0.60	0.33	0.19
GR-6	7.75(22)	0.25(19)	0.56(13)	0.65(19)	3.04(33)	0.54	0.38	0.61	0.47	0.67	0.33
GR-7	8.00(16)	0.08(8)	0.71(25)	0.63(13)	2.77(54)	0.47	0.30	0.43	0.47	0.70	0.33
GR-8	7.93(10)	0.07(9)	0.52(11)	0.64(7)	3.21(19)	0.55	0.41	0.71	0.47	1.13	0.45
GR-9	7.86(20)	0.15(18)	0.37(18)	0.74(20)	3.22(53)	0.67	0.43	0.75	0.63	1.17	0.46

Notes: The compositional variables x, y refer to the palygorskite formula $y[Mg_5Si_8O_{20}(OH)_2 \cdot (1-y)[x Mg_2Fe_2 \cdot (1-x)Mg_2Al_2]Si_8O_{20}(OH)_2$. K_{NIR} is the intensity of the Mg_3OH stretching overtone divided by the sum intensity of its dioctahedral AlAlOH, AlFeOH, and FeFeOH counterparts.
* AEM data from Suárez et al. (2007).

of trioctahedral-like magnesian palygorskite can approach 50% (ESQ-2 and GR-9).

The evaluation of the samples by NIR indicates that the only OH stretching overtones observed are the Al-Fe dioctahedral-like triplet (AlAlOH: 7056 cm^{-1}, $AlFe^{3+}OH$: 6994 cm^{-1}, and $Fe^{3+}Fe^{3+}OH$: 6928 cm^{-1}) and the Mg_3OH trioctahedral-like component at 7214 cm^{-1}. The relative intensities of the three dioctahedral-like components plotted in a ternary diagram (Fig. 2) confirm the location of palygorskite on a depressed compositional arc (Gionis et al. 2007), but with new data points plotting near the AlAlOH limit. These normalized intensities (I_{AlAlOH} + I_{AlFeOH} + I_{FeFeOH} = 1) are used to estimate $x = I_{FeFeOH} + ½I_{AlFeOH}$ from the NIR data (Table 1), with the assumption (Gionis et al. 2007) that the corresponding modes exhibit identical extinction coefficients. The values of x calculated independently from the AEM and NIR experiments are in excellent agreement within a narrow error bar (Fig. 3). This result is significant because it indicates that all Al and Fe assigned to octahedral sites by AEM, participate solely in the formation of the M2M2OH species: AlAlOH, $AlFe^{3+}OH$, and $Fe^{3+}Fe^{3+}OH$.

Although Figure 3 indicates that the effective extinction coefficients of the three $(Al,Fe^{3+})OH$ stretching overtone modes are identical, and therefore their sum intensity is proportional to $(1 - y)$, the same is not true for the Mg_3OH overtone. The relative intensity of the Mg_3OH vs. summed $(Al,Fe^{3+})OH$ overtone components, K_{NIR}, can yield $y/(1 - y)$ after calibration against data derived from AEM (Table 1). The K_{NIR} is linearly related to $y/(1 - y)$ with a correlation coefficient $R^2 = 0.88$ and a slope $\varepsilon = 1.38 \pm 0.08$ (graph not shown), where ε represents the relative extinction coefficient of the trioctahedral-like vs. dioctahedral-like OH overtones and is dependent on the specific NIR spectral acquisition (resolution) and analysis parameters (apodization, zero-filling, and smoothing factors). Using the 1.38 value for ε, a value for $y_{NIR} = K_{NIR}/(\varepsilon + K_{NIR})$ can be calculated from the NIR data, and compared to $y = [2Mg - 2(Al + Fe)]/[2Mg + 3(Al + Fe)]$ derived from the AEM data. This regression (Fig. 4) provides a NIR estimation of the trioctahedral-like fraction of palygorskite. This fraction ranges from $y = 0$ (precisely dioctahedral) to ca. 0.50 with a standard deviation of 0.05.

This study sets new limits on the composition of palygorskite, especially on the Fe-rich side of the plot (Fig. 2). Bulk samples with $x \leq 0.70$ were identified in the Pefkaki deposit (Gionis et al. 2007), whereas the AEM analysis of one sample (GR-9) has revealed single particles with an x value approaching 0.90. Therefore, the existence of palygorskite with x ranging continuously from 0 to 1 cannot be precluded. Furthermore, this study confirms that the fraction of trioctahedral-like palygorskite, y, is not correlated with Fe content. An upper limit of $y \approx 0.50$ is

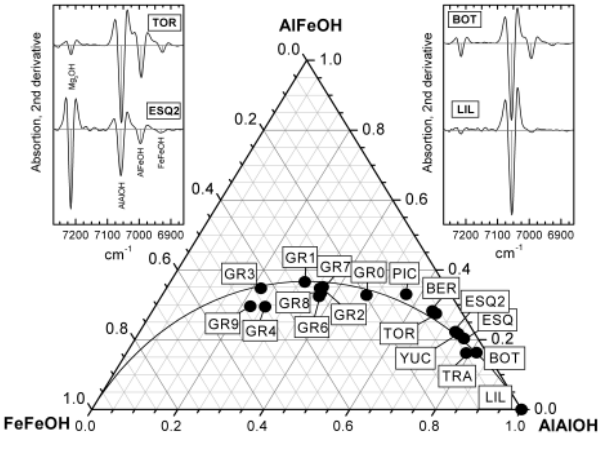

FIGURE 2. Occupancy of the M2M2OH groups of palygorskite by AlAl, $AlFe^{3+}$, and $Fe^{3+}Fe^{3+}$ pairs as in Gionis et al. (2007). Insets show details of the second derivative OH overtone spectra of selected samples and define how intensities have been measured.

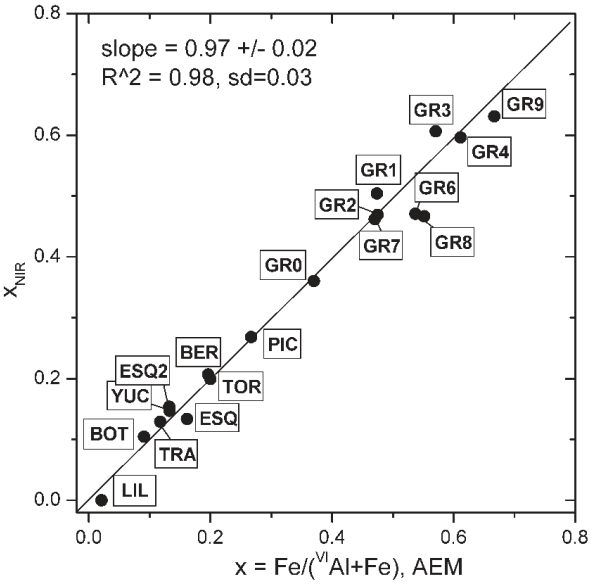

FIGURE 3. Fe^{3+} occupancy in the M2 sites of palygorskite estimated by NIR vs. the octahedral Fe/(Al + Fe) ratio measured by AEM. The line is a least-squares fit.

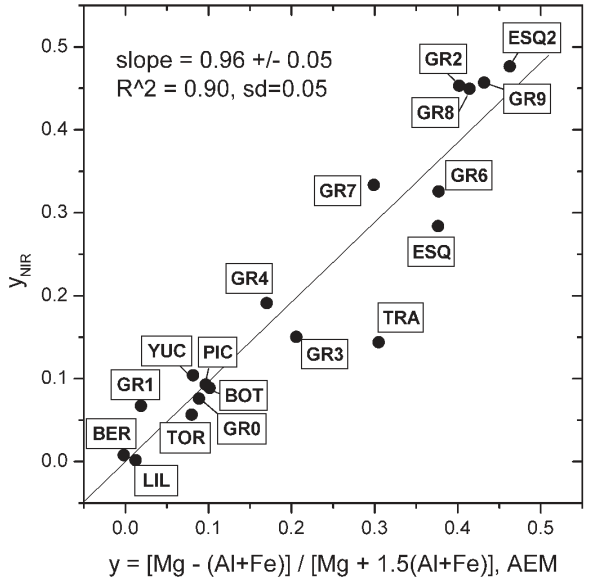

FIGURE 4. Fraction of trioctahedral magnesian palygorskite estimated by NIR and AEM. The line is a least-squares fit.

observed in bulk palygorskites with low (ESQ-2), intermediate (GR-2, Gr-8), or high (GR-9) values of x. Particles with widely variable y were determined in these samples by AEM (e.g., $0.11 < y < 0.68$ in ESQ-2), but precisely trioctahedral palygorskite particles ($y = 1$) were not found.

The agreement between the spectroscopic and analytical data validates the simplified palygorskite formula of Gionis et al. (2007) and demonstrates the capabilities of NIR for the fast and accurate evaluation of the composition of palygorskite with virtually no sample preparation. The determination of the Fe content, x, in dioctahedral palygorskite is particularly simple and can be biased only if significant crystalline dioctahedral phyllosilicates (e.g., kaolinite) are present in the sample. The determination of y is less straightforward and depends on the assumption that the relative extinction coefficient of the trioctahedral-like vs. dioctahedral-like OH stretching overtones is constant.

Acknowledgments

Funding for this work has been provided by Geohellas S.A. (NHRF) and the Spanish CICYT (project CGL2006-09843). Steve Guggenheim and an anonymous reviewer are thanked for their valuable comments.

References cited

Cai, Y., Xue, J., and Polya, D.A. (2007) A Fourier transform infrared spectroscopic study of Mg-rich, Mg-poor, and acid leached palygorskites. Spectrochimica Acta Part A, 66, 282–288.

Chahi, A., Petit, S., and Decarreau, A. (2002) Infrared evidence of dioctahedral-trioctahedral site occupancy in palygorskite. Clays and Clay Minerals, 50, 306–313.

Galán, E. and Carretero, I. (1999) A new approach to compositional limits for sepiolite and palygorskite. Clays and Clay Minerals, 47, 399–409.

García-Romero, E., Suárez, M., Santarén, J., and Alvarez, A. (2007) Crystallochemical characterization of the palygorskite and sepiolite from the Allou Kagne deposit, Senegal. Clays and Clay Minerals, 55, 606–617.

Gionis, V., Kacandes, G.H., Kastritis, I.D., and Chryssikos, G.D. (2006) On the structure of palygorskite by mid- and near-infrared spectroscopy. American Mineralogist, 91, 1125–1133.

——— (2007) Combined near-infrared and X-ray diffraction investigation of the octahedral sheet composition of palygorskite. Clays and Clay Minerals, 55, 543–553.

Giustetto, R. and Chiari, G. (2004) Crystal structure refinement of palygorskite from neutron powder diffraction. European Journal of Mineralogy, 16, 521–532.

Paquet, H., Duplay, J., Valleron-Blanc, M.M., and Millot, G. (1987) Octahedral compositions of individual particles in smectite-palygorskite and smectite-sepiolite assemblages. In L.G. Schultz, H. van Olphen, and F.A. Mumpton, Eds., Proceedings of the International Clay Conference, 1985, p. 73–77. The Clay Minerals Society, Bloomington, Indiana.

Post, J.E. and Heaney, P.J. (2008) Synchrotron powder X-ray diffraction study of the structure and dehydration behavior of palygorskite. American Mineralogist, 93, 667–675.

Serna, C., VanScoyoc, G.E., and Ahlrichs, J.L. (1977) Hydroxyl groups and water in palygorskite. American Mineralogist, 62, 784–792.

Singer, A. (1989) Palygorskite and sepiolite group minerals. In J.B. Dixon and S.B. Weed, Eds., Minerals in Soil Environments No. 1, Ch. 17, p. 829–872. Soil Science Society of America (SSSA) Book Series, Madison, Wisconsin.

Suárez, M. and García-Romero, E. (2006) FTIR spectroscopic study of palygorskite: Influence of the composition of the octahedral sheet. Applied Clay Science, 31, 154–163.

Suárez, M., García-Romero, E., Sánchez del Río, M., Martinetto, P., and Dooryhée, E. (2007) The effect of octahedral cations on the dimensions of the palygorskite cell. Clay Minerals, 42, 287–297.

Van Olphen, H. (1966) Maya Blue: A clay-organic pigment? Science, 154, 3749, 645–646.

Manuscript received August 1, 2008
Manuscript accepted September 22, 2008
Manuscript handled by Bryan Chakoumakos